Renewable and Sustainable Energy Reviews 132 (2020) 110151

Contents lists available at ScienceDirect

Renewable and Sustainable Energy Reviews

journal homepage: http://www.elsevier.com/locate/rser

Optimizing wind/solar combinations at finer scales to mitigate renewable energy variability in China

Laibao Liu [a,b,k], Zheng Wang [a], Yang Wang [b,**], Jun Wang [c], Rui Chang [b], Gang He [d], Wenjun Tang [e,f], Ziqi Gao [g], Jiangtao Li [h], Changyi Liu [i], Lin Zhao [j], Dahe Qin [a], Shuangcheng Li [a,*]

[a] College of Urban and Environmental Sciences, Peking University, Beijing, 100871, China
[b] National Climate Center, China Meteorological Administration, Beijing, 100081, China
[c] Key Laboratory for Human and Environmental Science and Technology, Peking University Shenzhen Graduate School, Shenzhen, 518055, China
[d] Department of Technology and Society, College of Engineering and Applied Sciences, Stony Brook University, Stony Brook, New York, 11794, United States
[e] Key Laboratory of Tibetan Environment Changes and Land Surface Processes, Institute of Tibetan Plateau Research, Chinese Academy of Sciences, Beijing, 100101, China
[f] CAS Center for Excellence in Tibetan Plateau Earth Sciences, Chinese Academy of Sciences, Beijing, 100101, China
[g] Gold wind Science and Technology CO., LTD, Beijing, 100176, China
[h] State Grid Energy Research Institute, Beijing, 102209, China
[i] Global Energy Interconnection Development and Cooperation Organization, Beijing, 100031, China
[j] China General Certification, Beijing, 100013, China
[k] Institute for Atmospheric and Climate Science, ETH Zurich, Zürich, 8006, Switzerland

ARTICLE INFO

Keywords:
Wind energy
Solar energy
Energy stability
Install ratio
Spatial aggregation
China

ABSTRACT

China has set ambitious goals to cap its carbon emissions and increase low-carbon energy sources to 20% by 2030 or earlier. However, wind and solar energy production can be highly variable: the stability of single wind/solar and hybrid wind-solar energy and the effects of wind/solar ratio and spatial aggregation on energy stability remain largely unknown in China, especially at the grid cell scale. To address these issues, we analyzed the newly 2007–2014 hourly wind and solar data, which have higher resolution and quality than those used in previous research. The stability of single wind/solar energy production clearly increased as the wind/solar energy capacity factor increased, and there were significant functional relationships between single wind/solar energy stability and the wind/solar energy capacity factor. Highly stable wind energy was concentrated in eastern Inner Mongolia, northeastern China, and northern China while highly stable solar energy was concentrated in the Tibetan Plateau, Inner Mongolia, and northwestern China. Different wind/solar ratios affected the stability of hybrid wind-solar energy through a unimodal relationship, allowing us to produce a map of optimal wind/solar ratios throughout China in order to minimize the variability of hybrid wind-solar energy production. At the optimal wind/solar ratio, the most stable hybrid wind-solar energy was concentrated in eastern Inner Mongolia, northeastern China, and northern China. The variability of single and hybrid wind/solar energy decreased as the aggregated area size increased, especially for wind-dominated energy systems. These results have important practical applications: (a) using the optimal wind/solar ratio to install simple hybrid wind-solar energy systems locally; (b) prioritizing the deployment of large-scale wind farms or centralized solar photovoltaic stations in regions with high hybrid energy stability; and (c) strongly promoting regional cooperation, such as breaking inter-provincial power grid barriers, to reduce the variability of hybrid wind-solar energy production and thus operational costs.

* Corresponding author. College of Urban and Environmental Sciences, Peking University, No.5 Yiheyuan Road, Haidian District, Beijing, 100871, China.
** Corresponding author. National Climate Center, China Meteorological Administration, No.46 Zhongguancun South Avenue, Haidian District, Beijing, 100081, China.
E-mail addresses: wangyang@cma.gov.cn (Y. Wang), scli@urban.pku.edu.cn (S. Li).

https://doi.org/10.1016/j.rser.2020.110151
Received 16 October 2019; Received in revised form 25 May 2020; Accepted 23 July 2020

Nomenclature

CMA	China Meteorological Administration
CAS	Chinese Academy of Sciences
NCC	National Climate Center
CF	The capacity factor
CF_{wind}	The capacity Factor of wind
CF_{solar}	The Capacity Factor of soalr
ANN	Artificial Neural Network
MODIS	Moderate Resolution Imaging Spectroradiometer
MTSAT	Multifunctional Transport Satellite
GLASS	Global Land Surface Satellite
ISCCP-FD	International Satellite Cloud Climatology Project F-Series of Products
P_{pv}	The actual solar photovoltaic power output
$P_{PV,STC}$	The rated power of the PV array under standard test conditions
$\eta_{PV,STC}$	The efficiency of the PV array under standard test conditions
μ	The temperature coefficient of the output power
STC	The standard test conditions
T_a	The ambient temperature
T_{STC}	The standard test conditions temperature
ν	The wind speed
NOCT	The nominal operating cell temperature
A_{PV}	The PV array areas (m^2) related to the PV array power peak
$G_{g,t}$	The global solar radiation on the titled surface
R_{STC}	The solar light intensity under standard test conditions
K	The ratio of the optimal slope total irradiance to the global horizontal irradiance
α	The system efficiency coefficient
CV	The coefficient of variation
$Instab_{energy}$	The instability of an energy system
$Instab_{wind}$	The single wind energy system instability
$Instab_{solar}$	The single solar energy system instability
u_E	The average energy generated in a year
T	The total number of hours in a year
i	The time step
E_i	The energy generated at time i
m	The weights of the wind CF
n	The weights of the solar CF

1. Introduction

The decarbonization of electrical power is a key requirement for reducing carbon dioxide emissions, mitigating climate change, and achieving sustainable developments [1,2]. Although China is the world's largest greenhouse gas emitter and energy consumer, at the 2015 United Nations Climate Change Conference it pledged to cap its carbon emissions and increase low-carbon energy to 20% of its total primary energy mix by 2030 or earlier [1,3]. This means that more renewable energy resources will be integrated into Chinese power systems, especially wind and solar. According to a report from the Energy Research Institute National Development and Reform Commission of China, ~2.4 billion kW of wind power and 2.7 billion kW of solar power are projected to be installed by 2050 with a total annual output of 9.66 trillion kWh, accounting for 64% of China's total power generation [4]. Wind and solar will, therefore, become the main sources of green

Table 1
Overview of datasets used in previous main wind/solar energy and hybrid wind-solar synergy assessments in China.

	Reference	Study area	Study period	Data sources	Spatial resolution	Time resolution	Wind speed height	Validation against wind masts	Validation against radiation station
Wind energy assessments	[7]	China	2001–2010	200 sites from 3TIER (https://www.3tier.com/)	Site scale	Hourly	100 m (onshore)	No	–
	[8]	China	1979–2015	MEERA (https://gmao.gsfc.nasa.gov/reanalysis/)	~56 × 61 km	Hourly	80 m (onshore), 120 m (offshore)	No	–
	[5]	China	1998–2017	MEERA-2 (https://gmao.gsfc.nasa.gov/reanalysis/)	~56 × 57 km	Hourly	50 m (onshore)	No	–
	[9]	China	2006–2015	2430 meteorological sites from CMA (http://data.cma.cn/)	Site scale	6-hourly	10 m (onshore)	–	–
	This study	China	2007–2014	CMA WRF simulation	15 × 15 km	Hourly	100 m (onshore)	Yes	–
Solar energy assessments	[10]	China	2001–2010	200 sites from 3TIER	Site scale	Hourly	–	–	Yes
	[6]	China	1970–2000	WorldClim (https://www.worldclim.org/)	1 × 1 km	Monthly	–	–	Yes
	This study	China	2007–2014	CAS Satellite-based model	5 × 5 km	Hourly	–	–	Yes
Wind-Solar synergy assessments	[26]	China	2009–2010	22 meteorological sites	Site scale	Hourly	10 m	No	Yes
	[24]	China	1971–2003	289 meteorological sites from Standard Meteorological Database for Buildings	Site scale	Daily	10 m	No	Yes
	[25]	Shandong Province	2006–2015	MEERA	~56 × 61 km	Hourly	50 m	No	No
	This study	China	2007–2014	CMA WRF simulation (wind); CAS Satellite-based model (Solar)	15 × 15 km (wind); 5 × 5 km(solar)	Hourly	100 m	Yes	Yes

Note: '-' indicates data not provided or not relevant.

electricity in China.

Many studies have conducted initial assessments of wind and solar resources within China as a necessary precursor to utilization [5,6]. Wind energy assessments primarily use reanalysis data sets (such as MERRA-2 and ERA-Interim) and meteorological station observations [7,8]. However, wind speeds from reanalysis data sets are not usually validated against wind mast data, while meteorological stations only measure the near-surface wind speed (at 10 m altitude), which needs to be adjusted to the wind turbine hub height (typically 70–100 m), creating large uncertainties [9]. Solar energy assessments typically rely on solar radiation observations from meteorological stations [6,10], but less than 100 radiation stations are operational in China, too few to accurately represent regional solar characteristics. Interpolating this limited network over China as a whole inevitably introduces large uncertainties. Recently, however, high-quality wind profile data from the China Meteorological Administration (CMA) and solar radiation data developed by the Chinese Academy of Sciences (CAS) have become available, allowing more precise assessments of potential wind and solar energy resources (See Table 1 for a detailed review on the wind/solar datasets mainly used in previous studies).

Power systems require a stable and continuous electricity supply, but wind and solar energy are inherently intermittent and unstable [11,12]. Potential mismatches between renewable energy supplies and load demands create clear challenges for integrating these resources into existing power grids. China's curtailment rate for wind and solar power generation has averaged over about 10% during the past decade, far higher than the 1–4% average curtailment rate in the United States and Europe. For example, from 2010 to 2016, 150.4 million MWh of renewable electricity generation were abandoned in China, a total energy loss equivalent to 48 million t of coal consumption or 134 million t of CO_2 emissions, representing ~1.5% of China's total emissions in 2016 [13]. In addition, such curtailments increase the Levelized cost of electricity, power system operation costs, and congestion management costs, while reducing the incomes of wind and solar farms [12,14].

Fortunately, a growing body of research has indicated that solar and wind are temporally complementary to some degree and together can increase the stability of a hybrid wind-solar energy system relative to either alone [15,16]. For instance, implementing integrated wind and solar power decreased the variability of power production in Ontario, Canada [17]; similar analyses have been conducted in Poland [18], West Africa [19], Iberian Peninsula [20], Britain [21], Australia [22], and the US [23]. Hence, energy systems that are highly dependent on wind and solar resources should assess the stability of hybrid wind-solar energy before deploying energy infrastructure.

Recent studies have begun to assess the potential for stable hybrid wind-solar energy systems in China [24,25]. For example, Liu et al. [26] found that combining wind and solar powers with a certain area can decrease zero-power hours in several Chinese provinces using data from 22 meteorological sites. Xu et al. [24] found that wind and solar are strongly complementary in North and Northwest China, using 289 meteorological sites. Zhang et al. [25] found that optimal use of wind and solar together can smooth aggregated power and decrease the power variability in Shandong Province based on MERRA reanalysis data. In addition, aggregating larger areas of wind farms and photovoltaic power stations can effectively reduce the variability of energy production [23,27]. For instance, in England [28], Denmark [29], Europe [30], the US [31], and Canada [32], the variability of hourly wind power decreases exponentially as the aggregated areas grow. A similar pattern has been documented for solar in the US [33] and Japan [34].

However, similar studies in China have suffered from certain limitations in that they: (1) have not assessed the variability of single wind/solar and hybrid wind-solar energy throughout China at the grid cell scale (the area of one grid cell is 15 × 15 km^2); (2) have not considered the wind/solar ratio's effect on hybrid wind-solar energy stability; and (3) have not investigated the effects of spatial aggregation on hybrid wind-solar energy stability. To address these shortcomings, in this study, we used the new high-quality wind and solar energy data from the CMA and CAS to determine:

(1) the stability of single wind/solar energy in China at the grid cell scale;
(2) the influence of the wind/solar ratio on the stability of hybrid wind-solar energy in China and the optimal ratio for stability;
(3) the influence of spatial aggregation on the stability of single wind/solar and hybrid wind-solar energy in China and the effect of the wind/solar ratio on this dynamic.

2. Data and methods

2.1. Wind energy assessment

Wind profile data were obtained from the CMA's National Climate Center (NCC), which assimilated data from Fengyun meteorological satellites, ~2400 ground stations, and 169 sounding stations before using a mesoscale numerical simulation model (the Weather Research and Forecasting Model) to produce hourly wind speed, wind direction, air density, and other variables from 1995 to 2016 [35]. These data have a horizontal resolution of 15 × 15 km. The wind profile altitude ranges from 10 to 200 m with 10 m vertical resolution. Independent validation against data from 400 wind masts at 70–120 m height built by CMA showed that these data have higher accuracy and quality than the commonly used MERRA-2 and ERA5 global reanalysis data in China [35].

We based this study on four mainstream onshore wind turbine types (GW131–2.2, GW121–2.0, GW140–3.4, and GW109–2.5; Goldwind, China) with 100 m hub heights (Table 2). These were chosen with reference to regional differences in multi-year average wind speed based on recommendations from the manufacturer, which accounted for 31.7% of China's wind energy market in 2018 [36]. The spatial distribution of suitable onshore wind turbine types is shown in Fig. 1a. The theoretical wind power was calculated using hourly wind speed, air density, and specific wind turbine power curves (Fig. 1b). The actual wind power equals the theoretical wind power multiplied by a system efficiency coefficient, which usually ranges between 20 and 30% [37]; we used the average value (25%).

The capacity factor (CF), which refers to the ratio of actual electricity generation over a year to the maximum possible electricity generation over that year was calculated as:

$$CF = \frac{\text{Annual power generation (MWh)}}{\text{Installed capacity (MW)} \times \text{Hours in a year (h)}} \quad (1)$$

2.2. Solar energy assessment

The CAS satellite-based surface solar radiation data have 5 × 5 km spatial resolution and hourly temporal resolution from 2007 to 2014. This data set was produced using an artificial neural network(ANN)-based algorithm built by combining Moderate Resolution Imaging Spectroradiometer (MODIS) cloud products and Multifunctional Transport Satellite (MTSAT) data to estimate cloud parameters (cloud mask, effective particle radius, and liquid/ice water path) from MTSAT imagery [38]. The estimated cloud parameters and other information (such

Table 2
Turbine parameters and wind speed ranges.

Average wind speed range (m/s)	Turbine type	Capacity (MW)	Rotor diameter (m)
4.5–6.5	GW131–2.2	2.2	131
6.5–7.5	GW121–2.0	2.0	121
7.5–8.5	GW140–3.4	3.4	140
>8.5	GW109–2.5	2.5	109

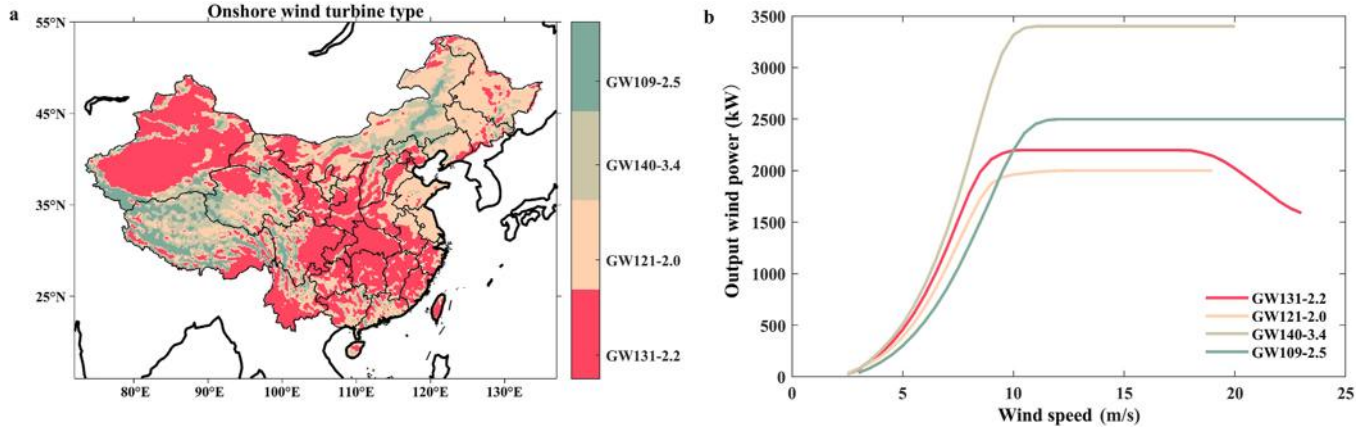

Fig. 1. (a) Spatial distribution of suitable onshore wind turbine types based on multi-year averaged wind speed. (b) Example generating power curves of four onshore wind turbines with a standard air density of 1.225 kg/m^3.

as aerosols, ozone, and precipitable water) were entered into a parameterization model to calculate horizontal solar radiation. By independent validation against both experimental data and operational station data in China, the accuracy and quality of these data were determined to be comparable to or higher than two commonly used solar radiation products (GLASS and ISCCP-FD) with coarser spatial resolution [38]. The solar energy data were then bilinearly gridded to match the spatial resolution of the wind energy data.

The actual solar photovoltaic power output was calculated using an open-source package, OptiCE [39,40], which was widely used in PV simulation [41,42]. The 3-hourly ambient temperature data was retrieved from ERA-interim reanalysis [43] and interpolated to an hourly scale. The hourly wind speed was obtained from CMA's National Climate Center. The hourly simulation of the PV system is calculated as follows:

$$P_{pv} = P_{PV,STC}\left[1 + \frac{\mu}{\eta_{PV,STC}}(T_a - T_{STC}) + \frac{\mu}{\eta_{PV,STC}}\frac{9.5}{5.7+3.8\nu}\frac{(NOCT-20)}{800}(1- \eta_{PV,STC}) \times G_{g,t}\right]\frac{G_{g,t}}{R_{STC}} \times A_{PV} \times K \times \alpha \quad (2)$$

where P_{pv} is the actual solar photovoltaic power output (W); $P_{PV,STC}$is the rated power of the PV array under standard test conditions; $\eta_{PV,STC}$is the efficiency of the PV array under standard test conditions (STC); μ is the temperature coefficient of the output power(%/°C); $T_a$is the ambient temperature (°C); $T_{STC}$is the standard test conditions temperature (25 °C);ν is the wind speed (m/s); NOCT is the nominal operating cell temperature (45 °C); A_{PV} is the PV array areas (m^2) related to the PV array power peak; $G_{g,t}$ is the global solar radiation on the titled surface (W/m^2); R_{STC} is the solar light intensity under the standard test conditions, and its value is 1000W/m^2; K is the ratio of the optimal slope total irradiance to the global horizontal irradiance. In this study, the optimal slope total irradiance at 2461 ground stations in China was calculated using the Klein-Hay model [44,45], and the K at the 2461 ground stations were spatially interpolated to get each value at each grid cell. α is the system efficiency coefficient, and its value is 0.8 [46]. Similar to the wind CF, the solar CF was then calculated as the ratio of actual solar PV electricity generation to solar PV potential electricity generation.

In summary, regarding the wind and solar data, there are 41137 spatial grid cells in China, and the data sets contain 78840 hourly time steps.

2.3. Hybrid wind-solar stability

2.3.1. Wind/solar install ratio

Instab$_{energy}$ is a standardized measure of the dispersion of energy production across time that can be used to compare instability in different locations and different energy systems. A lower Instab$_{energy}$ indicates that energy production is more stable and smoother over time. Following a previous study [19], we used the coefficient of variation (CV) to assess the instability of an energy system (Instab$_{energy}$):

$$Instab_{energy} = \frac{1}{u_E}\sqrt{\frac{1}{T}\sum_{i=1}^{T}(E_i - u_E)^2} \quad (3)$$

where u_E is the average energy generated in a year, T is the total number of hours in a year, i is the time step, and E_i is the energy generated at time i. In general, there are different combinations of wind-solar install ratio (m:n) such that a specific ratio can produce the lowest hybrid instability (Instab$_{hybrid}$). The optimal hybrid wind-solar energy with highest stability can thus be determined by boundary constraints:

$$Min\left(Instab_{hybrid}\right) \; such \; that \begin{cases} Instab_{hybrid} = CV(m \times CF_{wind} + n \times CF_{solar}) \\ m > 0,\ n > 0 \end{cases} \quad (4)$$

To better illustrate this method, considering a single grid cell (21.9 °N, 107.8 °E) as an example. To simplify the calculation, we assume a wind/solar install ratio of m : 1, which produces a relationship between Instab$_{hybrid}$ and wind/solar ratio in the form of a unimodal curve (Fig. 2). A wind/solar install ratio of 1.3:1 can thus result in the highest stability of hybrid wind-solar energy, i.e., the lowest Instab$_{hybrid}$.

2.3.2. Spatial aggregation

To assess the effect of spatial aggregation on the stability of hybrid wind/solar energy production, we applied a moving window strategy to ensure that the Instab$_{energy}$ at different spatial scales could be compared. For instance, in a 3 × 3 grid cell window (Fig. 3), the Instab$_{hybrid}$ is calculated as:

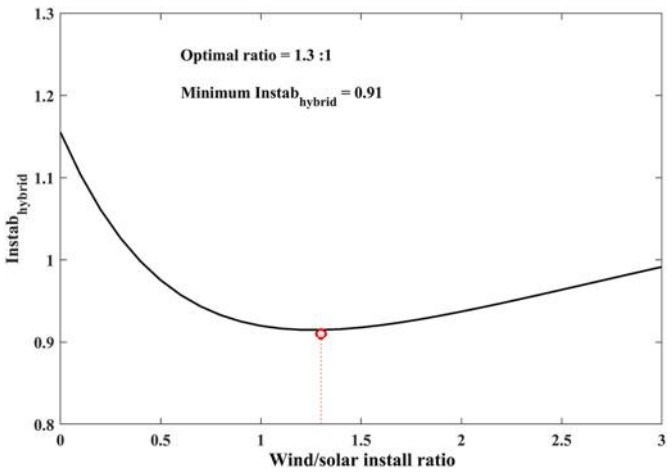

Fig. 2. Example of the relationship between hybrid wind-solar energy instability and the wind/solar install ratio. Red circle indicates the location of highest hybrid energy stability with an optimal wind/solar install ratio of 1.3:1. (For interpretation of the references to colour in this figure legend, the reader is referred to the Web version of this article.)

$$Instab_{hybrid} = CV\left(\sum_{i=1}^{N\times N} mCF_{wind,i} + \sum_{i=1}^{N\times N} nCF_{solar,i}\right) \quad (5)$$

where i represents the grid cell in a given grid cell window ($N \times N$) and m and n are the weights of the wind and solar CF. The central point of the grid cell window moves to the adjacent grid cell and the computations are repeated. We used grid cell windows of 1×1, 3×3, 9×9, 25×25, and 51×51. The area of one grid cell (i.e., 1×1) is 15×15 km^2.

3. Results

3.1. Wind and solar CF in China

High CF_{wind} was mainly distributed in Inner Mongolia, northeastern China, and northern China (Fig. 4). Compared with values determined at 80 m with a consistent turbine type in previous studies [7,8], those at 100 m were much higher, especially in northeastern and northern China. CF_{solar} was lower than CF_{wind} on average, consistent with previous studies [7,10]. High values were concentrated in western China, particularly in the Tibetan Plateau, while low values were concentrated in the Sichuan Basin due to frequent cloudy weather conditions.

3.2. Instability of single wind and solar energy

$Instab_{wind}$ showed large spatial heterogeneity, with an averaged value of 0.92 nationally (Fig. 5a); high values were concentrated in the Xinjiang and Sichuan Basins, where CF_{wind} was low, while low values were mostly distributed in eastern Inner Mongolia and northeastern China, where CF_{wind} was high. There was a clear negative and non-linear relationship ($Y = 2.12\, e^{-5.68X} + 0.48$, $R^2 = 0.91$) between $Instab_{wind}$ and CF_{wind} (Fig. 5c); the former decreased dramatically when the latter was <0.2 and decreased slowly when the latter was >0.2.

The spatial heterogeneity of $Instab_{solar}$ was lower than $Instab_{wind}$, but its values were much higher across most regions, averaging 1.44 (Fig. 5b). High values were concentrated in the Sichuan Basin, while low values were concentrated in the Tibet Plateau. There was a negative linear relationship between $Instab_{solar}$ and CF_{solar} ($Y = -1.9X + 1.76$, $R^2 = 0.79$) (Fig. 5d); in general, a 0.1 increase in the latter would produce a decrease of 1.9 in the former.

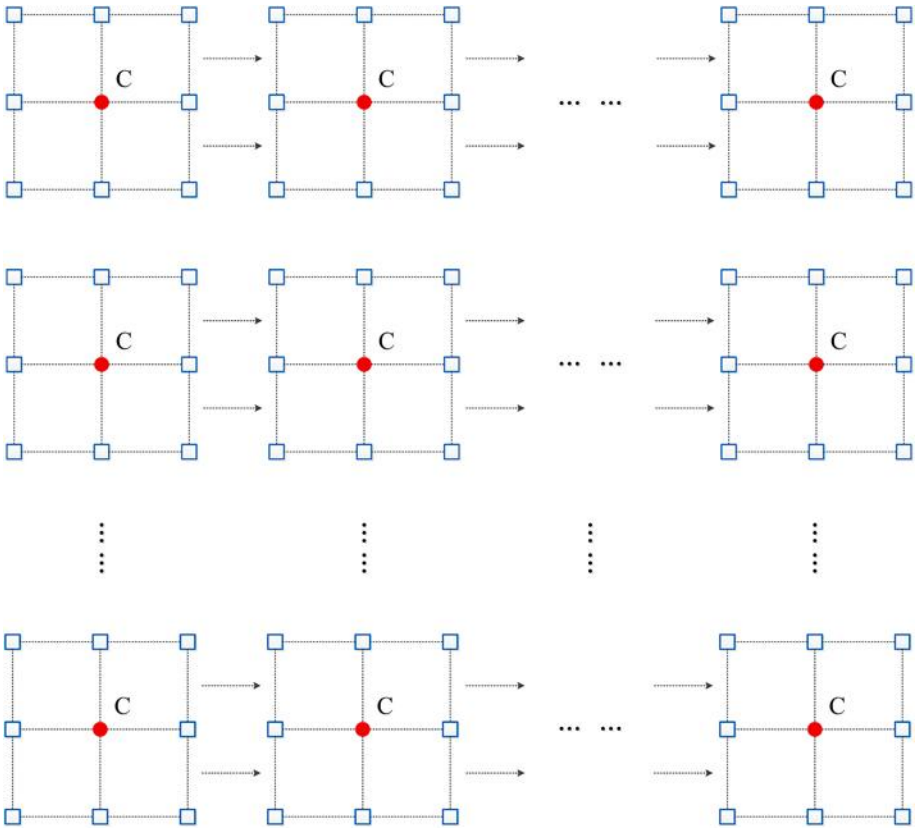

Fig. 3. Conceptual schematic of energy stability calculations in a 3×3 grid cell window. Red point C represents the central point of the 3×3 grid cell window; blue rectangle represents the 8 adjacent grid cells. (For interpretation of the references to colour in this figure legend, the reader is referred to the Web version of this article.)

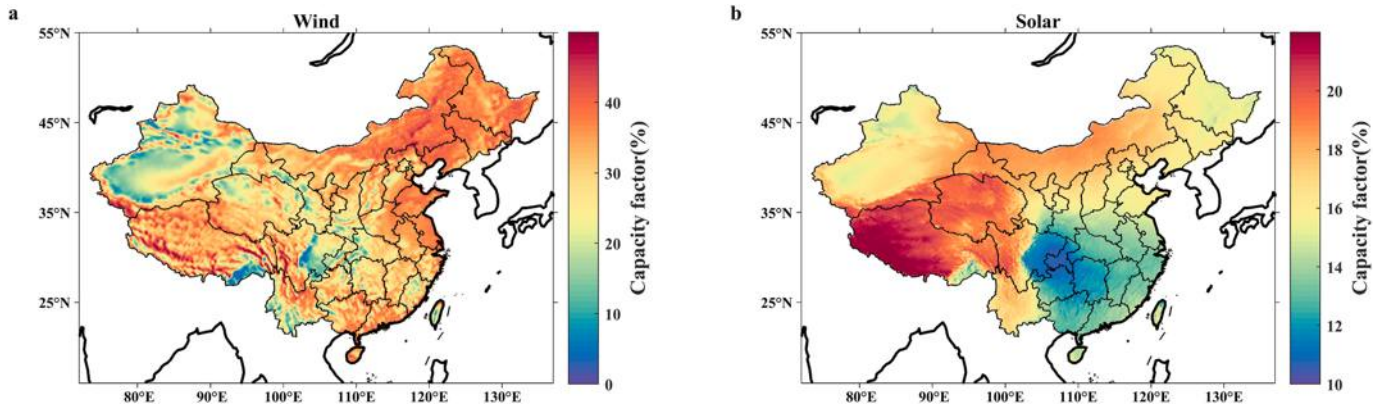

Fig. 4. Spatial distribution of averaged wind CF at 100 m altitude and solar CF in China from 2007 to 2014.

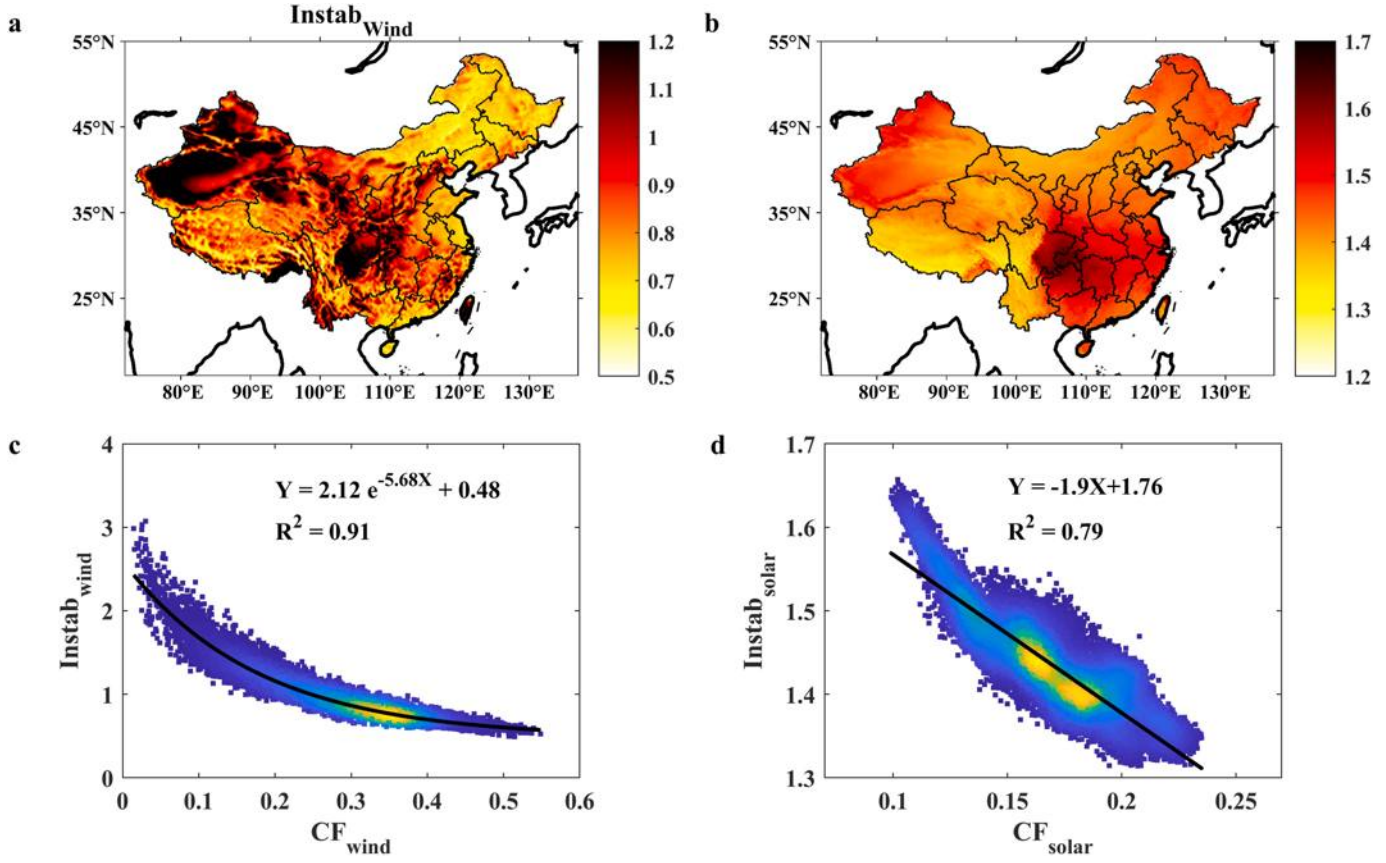

Fig. 5. Spatial distribution of averaged (a) single wind energy system instability ($Instab_{wind}$) and (b) single solar energy system instability ($Instab_{solar}$) in China during 2007–2014. Relationship between (c) $Instab_{wind}$ and CF_{wind} and (d) $Instab_{solar}$ and CF_{solar} in China during 2007–2014.

3.3. Effect of wind/solar install ratio on hybrid energy system stability

For hybrid wind/solar energy, $Instab_{hybrid}$ varied widely across different wind/solar install ratios (Fig. 6). Wind/solar install ratios of 1:0.5 and 1:1.5 induced the lowest $Instab_{hybrid}$ (averaged national values of 0.73 and 0.76, respectively) while a ratio of 1:3 induced the largest $Instab_{hybrid}$ (averaged national value of 0.91).

By computing the functional relationship between $Instab_{hybrid}$ and wind/solar install ratio per grid cell, we derived the lowest $Instab_{hybrid}$ and corresponding optimal install ratio (Fig. 7a,b). Compared with $Instab_{wind}$ and $Instab_{solar}$ alone (Fig. 5a and b) or hybrid wind/solar energy with a fixed ratio (Fig. 6), $Instab_{hybrid}$ was much lower, with an averaged national value of 0.70 (Fig. 7a and b). This suggests that integrating wind and solar with an optimal ratio can strongly decrease the instability of single and hybrid wind/solar energy production. The lowest $Instab_{hybrid}$ values for the optimal ratio were concentrated in high CF_{wind} regions, and the largest $Instab_{hybrid}$ values for the optimal ratio were mostly distributed in low CF_{wind} regions. We identified a strong negative relationship between $Instab_{hybrid}$ and CF_{wind} ($Y = 1.08e^{-3.11X}+0.26$, $R^2 = 0.88$, Fig. 7c), but the relationship between $Instab_{hybrid}$ and CF_{solar} was less well-defined (Fig. 7d).

Overall, the optimal wind/solar install ratio mostly ranged from 0.4:1 to 1.4:1. Thus, a high and low wind/solar ratio would increase the $Instab_{hybrid}$ in China. This is in line with the high $Instab_{hybrid}$ with wind/solar ratio of 1:0.1 and 1: 3 (Fig. 6a and d). The lowest ratios were concentrated in Inner Mongolia, northeastern China, and the Tibet

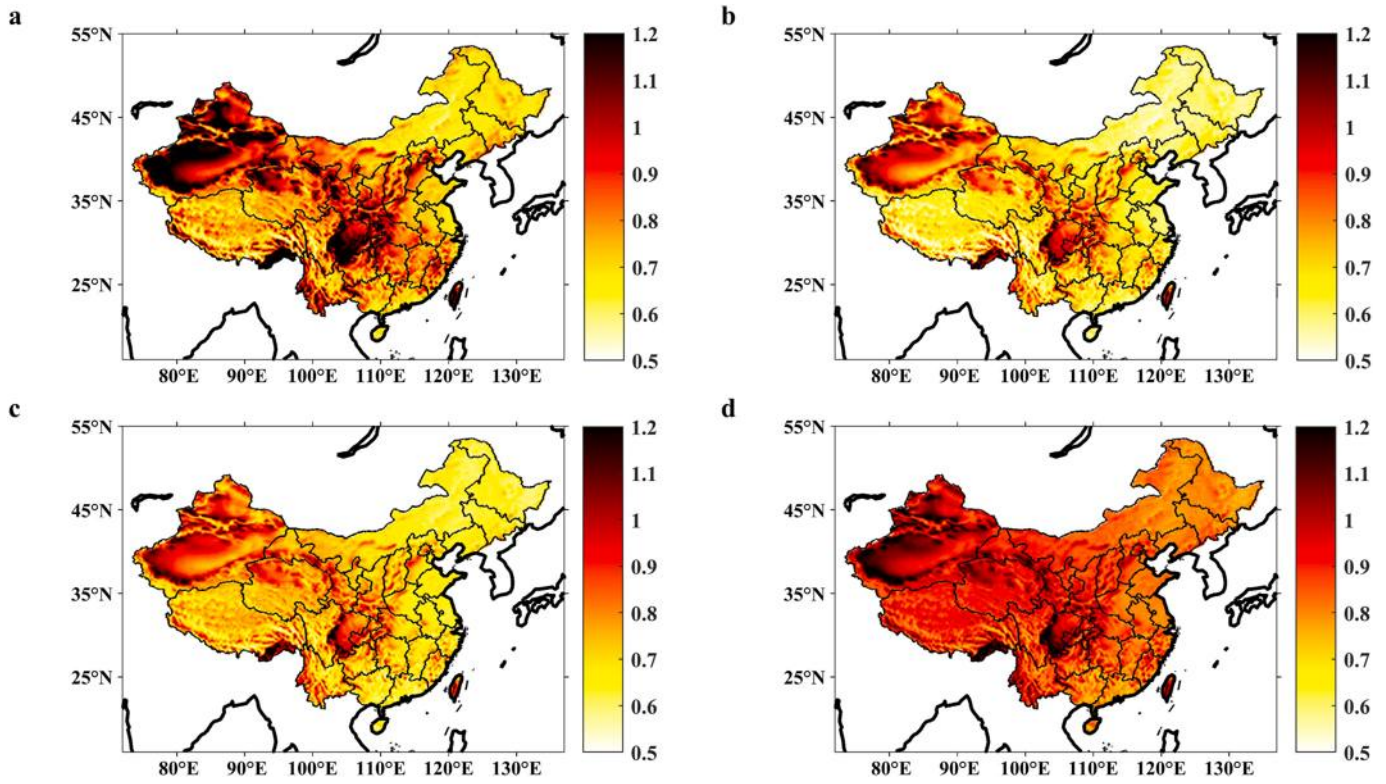

Fig. 6. Spatial distribution of averaged $Instab_{hybrid}$ with wind/solar install ratios of (a) 1:0.1, (b) 1:0.5, (c) 1:1.5, and (d) 1:3 in China during 2007–2014.

Plateau. The optimal install ratio did not seem to be correlated with CF_{wind} and CF_{solar} (Fig. 7e and f).

3.4. Effect of spatial aggregation on energy system stability

$Instab_{wind}$, $Instab_{solar}$, and $Instab_{hybrid}$ decreased in most areas, as the window size increased (Fig. 8). At 51×51, the spatial heterogeneity of the instability for all energy types became very low; $Instab_{wind}$ and $Instab_{hybrid}$ at wind/solar ratio of 1:1 decreased in most areas to ~0.5 and $Instab_{solar}$ to ~1.3. For single wind or solar energy, an increase in sliding window size from 1×1 to 51×51 reduced $Instab_{wind}$ by 45.7% but reduced $Instab_{solar}$ by only 7.5% (Fig. 9). For hybrid energy, the increase in window size had a larger effect on $Instab_{hybrid}$ with higher wind/solar ratio. For instance, $Instab_{hybrird}$ values at wind/solar ratios of 1:0.1 and 1: 3 were closer at 1×1, but when this increased to 51 × 51, $Instab_{hybird}$ at a wind/solar ratio of 1:0.1 decreased by 46.2% while $Instab_{hybrid}$ at a wind/solar ratio of 1:3 decreased by 13.6%. This suggests that larger spatial scales decrease wind/solar energy instability effectively, especially for wind-dominated hybrid wind-solar energy.

However, the effects of spatial aggregation on reducing energy instability are not linear. Increasing the window size from 1 × 1 to 9 × 9 (an increase of 1800 km^2) reduces $Instab_{wind}$ from 0.91 to 0.73, while increasing the window size from 25 × 25 to 51 × 51 (an increase of 4.5 $\times 10^5$ km^2) only reduces $Instab_{wind}$ from 0.62 to 0.5. In addition, the low differences in instability across multiple years indicated that the effects of spatial aggregation on energy system instability are robust with regard to the interannual variability of wind and solar energy.

4. Discussion and practical implications

This study assessed single wind/solar and hybrid wind-solar energy stability in China and the effects of the wind/solar ratio and spatial aggregation on energy stability. Compared with previous research, this study offers a more comprehensive and detailed assessment of these factors based on the new high-quality renewable energy data sets developed by the CMA and CAS. For example, previous analyses of wind-solar complementarity in China were mostly performed on the provincial or site scale [25,26], while no other studies have examined the wind-solar hybrid energy system stability at the grid cell scale throughout the country.

For single wind energy, the variability of wind energy decreases exponentially with CF_{wind}, while the variability of solar energy decreases linearly with CF_{solar}. This suggests that regions with rich wind resources (such as eastern Inner Mongolia, northeastern China, and northern China) and regions with rich solar resources (such as the Tibetan Plateau, Inner Mongolia, and northwestern China) have lower variability and are highly suitable for the development of large wind and solar installations. In addition, the variability of solar power is much higher that of wind power across most of China due to the diurnal cycle of solar radiation. Moreover, the significant functional relationships between CF and wind/solar instability mean that the instability of wind/solar energy can be estimated by using the wind/solar CF and our derived functions for a given location in China.

Unlike many previous studies of wind/solar synergy in China based on fixed wind/solar ratios [5,24], this study also explored the effects of varying wind/solar ratios on energy system stability. The optimal ratio turns out to be highly dependent on location, and an optimal wind/solar ratio can greatly improve the stability of hybrid wind-solar energy in China. The determination of an optimal wind/solar ratio is important for practical applications because this can minimize the variability of energy production and thus lower external system costs such as energy storage and grid integration.

At the optimal wind/solar ratio, the lowest instability for hybrid wind-solar energy is predominantly concentrated in eastern Inner Mongolia, northeastern China, and northern China, where wind resources are also abundant. Since the Chinese energy sector has planned several integrated multi-energy demonstration projects [46], we propose that large-scale wind-solar integration projects should be prioritized in these regions. A reasonable wind/solar install ratio for these projects could highly reduce the variability of power production and

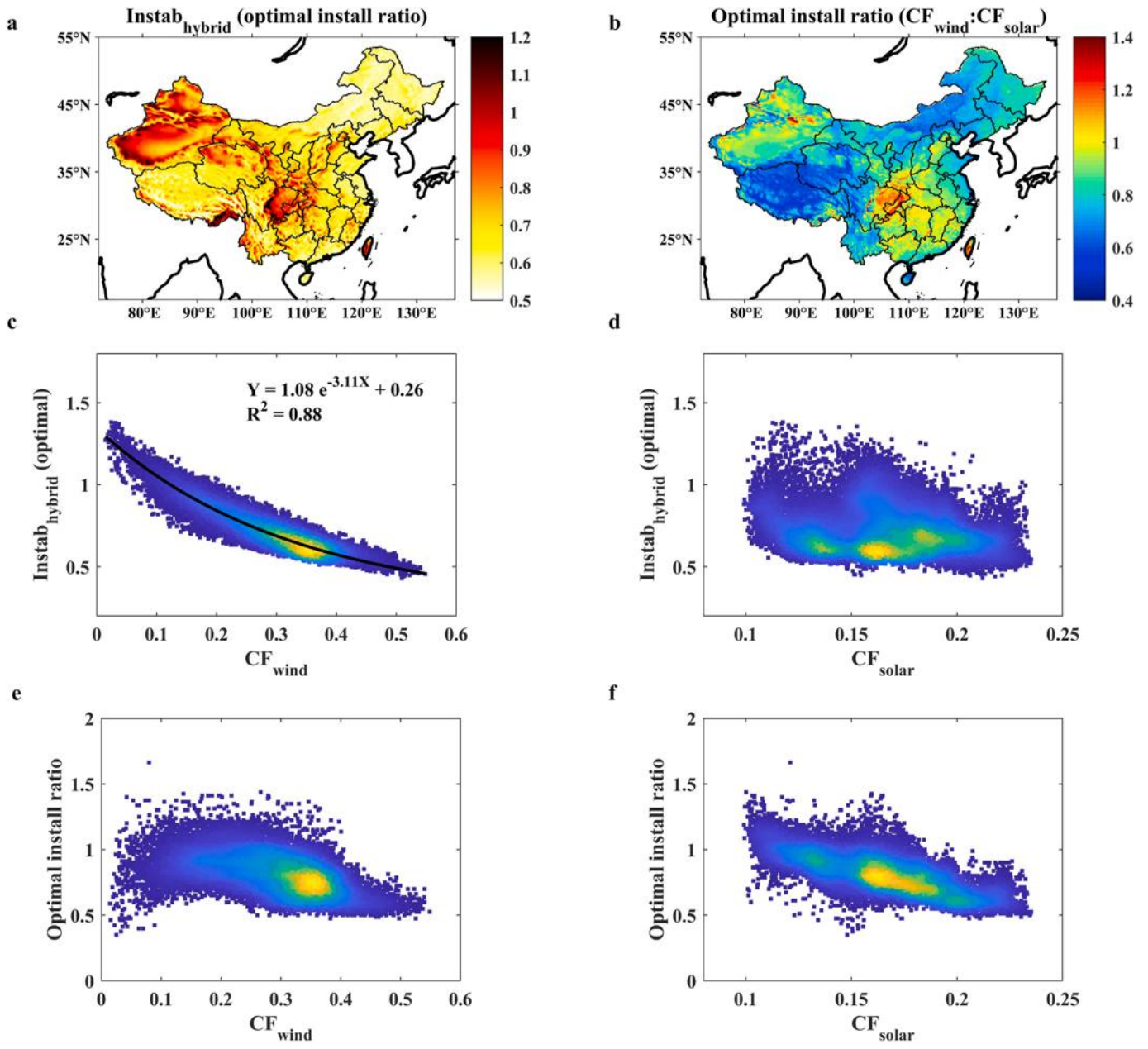

Fig, 7. Spatial distribution of (a) $Instab_{hybrid}$ for the optimal wind/solar ratio and (b) the optimal wind/solar ratio. Relationship between $Instab_{hybrid}$ and (c) CF_{wind} and (d) CF_{solar}. Relationship between optimal install ratio and (e) $Instab_{solar}$ and (f) CF_{solar} in China from 2007 to 2014.

thus improve the overall efficiency of renewable energy use, especially for industrial parks, public facilities, and business districts.

The fact that the variability of single wind/solar and hybrid energy systems decreases as the aggregated area increases, especially for wind-dominated energy systems, provides a solution for the problematic level of wind/solar curtailments in China that caused > $1.2 billion in opportunity costs from 2000 to 2016. In China, grid operating areas are generally set at the provincial scale where the variability of wind and solar resources is much higher relative to larger scales. Thus, excess electricity is likely to be generated during off-peak hours, resulting in curtailments of renewable energy [47]. However, at a larger scale, renewable energy variability is likely to be much lower, reducing the potential mismatch between demand and supply. Emphasizing regional cooperation, such as removing inter-provincial barriers, could improve grid operators' access to capacity reserve and demand, thus improving the system's ability to absorb wind/solar volatility and reducing operational costs [48]. Thus, the high-voltage transmission is a useful approach to aggregate these renewable energy, and the economic costs need to be further investigated. For solar-dominated systems, the effect of increased areas on reducing stability is much weaker, also in agreement with previous studies [23,27]. Thus, energy storage, demand management, and flexible generation could also be effective at reducing the variability of solar power production [23,27].

In this study, we focused on the two predominant renewable energy types (wind and solar) but did not consider others such as hydropower, bioenergy, natural gas, or energy storage. Future studies should explore other possible combinations of energy sources or energy storage to further improve the utilization of renewable energy and energy system stability [49,50]. In addition, with the rapid ongoing development of wind and solar energy technology, more abundant wind resources at higher altitudes can be gradually utilized, while dual-axis solar tracking systems and increases in solar cell efficiency can improve solar power generation [51]. These technical advancements could influence hybrid wind-solar system stability to an unknown degree, so future assessments

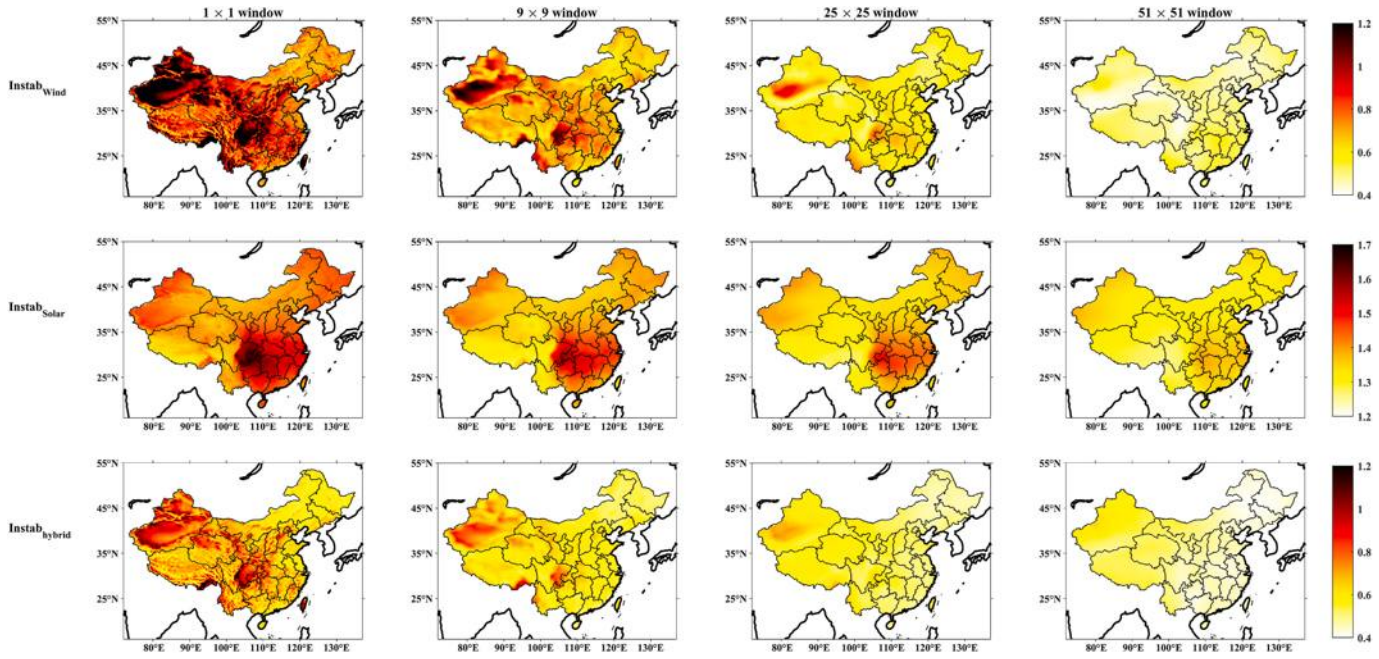

Fig. 8. Effect of spatial aggregation (window size) on $Instab_{wind}$, $Instab_{solar}$, and $Instab_{hybrid}$ at a wind/solar ratio of 1:1 in China from 2007 to 2014.

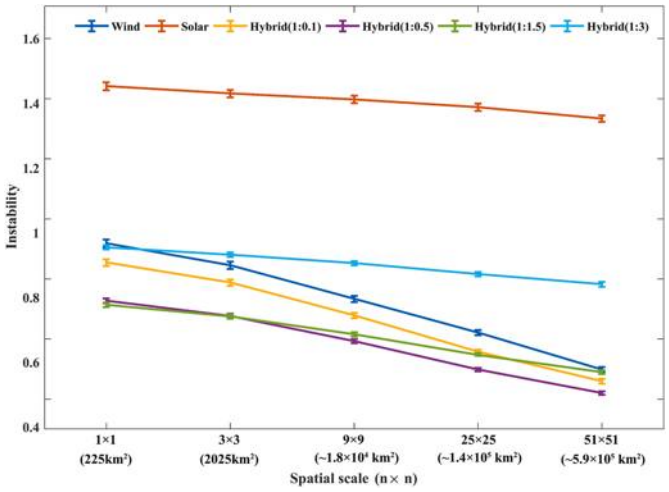

Fig. 9. Relationship between averaged $Instab_{wind}$, $Instab_{solar}$, and $Instab_{hybrid}$ with different wind/solar ratios and spatial scales in China from 2007 to 2014. Error bar shows the standard deviation of $Instab_{energy}$.

of wind/solar energy stability should be sure to consider current technological developments. It is also important to explore the potential to apply our methods and findings to similar challenges in other countries.

5. Conclusions

We used the high-quality hourly wind and solar radiation data recently released by China's CMA and CAS to assess the single wind/solar and hybrid wind-solar energy stability and effects of the wind/solar ratio and spatial aggregation on energy stability at the grid cell scale in China from 2007 to 2014.

The stability of single wind/solar energy production increased as the wind/solar energy capacity factor increased. Highly stable wind energy was predominantly concentrated in eastern Inner Mongolia, northeastern China, and northern China, while highly stable solar energy was mostly concentrated in the Tibetan Plateau, Inner Mongolia, and northwestern China. Furthermore, the significant functional relationships between wind/solar energy instability and wind/solar energy capacity can help approximate the instability of wind energy using the wind/solar CF and our derived functions at a given location in China ($Instab_{wind} = 2.96\ e^{-8.27CF_{wind}} + 0.7$and $Instab_{solar} = -2.54\ CF_{solar} + 1.92$).

For hybrid wind-solar energy, the choice of wind/solar install ratio can have large impacts on energy stability. Our map of optimal wind/solar install ratios provides a resource for minimizing the variability of hybrid wind-solar energy production and can guide the installation of simple hybrid wind-solar energy systems locally without the need for other energy sources.

Highly stable hybrid wind-solar energy was concentrated in eastern Inner Mongolia, northeastern China, and northern China, so these areas should be prioritized during Chinese government planning for the deployment of large-scale wind/solar farms. In addition, the variability of single wind/solar system and hybrid wind-solar energy decreased as the aggregated area increased, especially for wind-dominated hybrid wind-solar energy. This strongly suggests that promoting regional cooperation, such as breaking inter-provincial power grid barriers, can reduce the variability of wind-solar energy production, improve the system's ability to absorb wind/solar volatility, and reduce operational costs.

Declaration of Competing Interest

The authors declare that they have no known competing financial interests or personal relationships that could have appeared to influence the work reported in this paper.

CRediT authorship contribution statement

Laibao Liu: Conceptualization, Methodology, Formal analysis, Data curation, Writing - original draft. **Zheng Wang:** Methodology, Formal analysis, Writing - review & editing. **Yang Wang:** Conceptualization, Supervision, Writing - review & editing. **Jun Wang:** Writing - review & editing. **Rui Chang:** Writing - review & editing. **Gang He:** Writing - review & editing. **Wenjun Tang:** Writing - review & editing. **Ziqi Gao:** Writing - review & editing. **Jiangtao Li:** Writing - review & editing.

Changyi Liu: Writing - review & editing. **Lin Zhao:** Writing - review & editing. **Dahe Qin:** Writing - review & editing. **Shuangcheng Li:** Conceptualization, Supervision.

Acknowledgments

This work was supported by National Natural Science Foundation (Grant Number 41590843) and Shenzhen Science, Technology Innovation Committee Basic Research Funding Project (Grant Number JCYJ20180302150417674) and GEIGC Science and Technology Project (Grant Number 101662227). Laibao Liu was also funded by the China Scholar Council fellowship. The authors have no conflicts of interest to declare.

References

[1] Adoption of the Paris Agreement FCCC/CP/L.9/Rev.1. UNFCCC; 2015.
[2] Zeyringer M, Price J, Fais B, Li PH, Sharp E. Designing low-carbon power systems for Great Britain in 2050 that are robust to the spatiotemporal and inter-annual variability of weather. Nature Energy 2018;3:395–403.
[3] Jiang JJ, Ye B, Liu JG. Peak of CO2 emissions in various sectors and provinces of China: recent progress and avenues for further research. Renew Sustain Energy Rev 2019;112:813–33.
[4] Commission ERIoNDaR. China 2050 High Renewable Energy Penetration Scenario and Roadmap Study. Beijing: Tech. Rep.; 2015.
[5] Ren GR, Wan J, Liu JF, Yu DR. Characterization of wind resource in China from a new perspective. Energy 2019;167:994–1010.
[6] Yang Q, Huang TY, Wang SG, Li JD, Dai SQ, Wright S, et al. A GIS-based high spatial resolution assessment of large-scale PV generation potential in China. Appl Energy 2019;247:254–69.
[7] He G, Kammen DM. Where, when and how much wind is available? A provincial-scale wind resource assessment for China. Energy Pol 2014;74:116–22.
[8] Davidson MR, Zhang D, Xiong WM, Zhang XL, Karplus VJ. Modelling the potential for wind energy integration on China's coal-heavy electricity grid. Nature Energy 2016;1.
[9] Liu F, Sun FB, Liu WW, Wang TT, Wang H, Wang XM, et al. On wind speed pattern and energy potential in China. Appl Energy 2019;236:867–76.
[10] He G, Kammen DM. Where, when and how much solar is available? A provincial-scale solar resource assessment for China. Renew Energy 2016;85:74–82.
[11] MacDonald AE, Clack CTM, Alexander A, Dunbar A, Wilczak J, Xie YF. Future cost-competitive electricity systems and their impact on US CO2 emissions. Nat Clim Change 2016;6:526–31.
[12] Zhou S, Wang Y, Zhou YY, Clarke LE, Edmonds JA. Roles of wind and solar energy in China's power sector: implications of intermittency constraints. Appl Energy 2018;213:22–30.
[13] Ye Q, Jiaqi L, Mengye Z. Wind curtailment in China and lessons from the United States. China's Energy in Transition Series. Beijing, China: Brookings-Tsinghua Center for Public Policy; 2018. p. 4.
[14] Joos M, Staffell I. Short-term integration costs of variable renewable energy: wind curtailment and balancing in Britain and Germany. Renew Sustain Energy Rev 2018;86:45–65.
[15] Solomon AA, Kammen DM, Callaway D. Investigating the impact of wind-solar complementarities on energy storage requirement and the corresponding supply reliability criteria. Appl Energy 2016;168:130–45.
[16] Zhou W, Lou CZ, Li ZS, Lu L, Yang HX. Current status of research on optimum sizing of stand-alone hybrid solar-wind power generation systems. Appl Energy 2010;87:380–9.
[17] Hoicka CE, Rowlands IH. Solar and wind resource complementarity: advancing options for renewable electricity integration in Ontario, Canada. Renew Energy 2011;36:97–107.
[18] Jurasz J, Beluco A, Canales FA. The impact of complementarity on power supply reliability of small scale hybrid energy systems. Energy 2018;161:737–43.
[19] Sterl S, Liersch S, Koch H, van Lipzig NPM, Thiery W. A new approach for assessing synergies of solar and wind power: implications for West Africa. Environ Res Lett 2018;13.
[20] Jerez S, Trigo RM, Sarsa A, Lorente-Plazas R, Pozo-Vazquez D, Montavez JP. Spatio-temporal complementarity between solar and wind power in the Iberian Peninsula. In: Egudivision energy, resources & the environment, Ere. 2013, vol. 40. European Geosciences Union General Assembly; 2013. p. 48–57.
[21] Bett PE, Thornton HE. The climatological relationships between wind and solar energy supply in Britain. Renew Energy 2016;87:96–110.
[22] Prasad AA, Taylor RA, Kay M. Assessment of solar and wind resource synergy in Australia. Appl Energy 2017;190:354–67.
[23] Shaner MR, Davis SJ, Lewis NS, Caldeira K. Geophysical constraints on the reliability of solar and wind power in the United States (vol 11, pg 914, 2018). Energy Environ Sci 2018;11:997.
[24] Xu LJ, Wang ZW, Liu YF. The spatial and temporal variation features of wind-sun complementarity in China. Energy Convers Manag 2017;154:138–48.
[25] Zhang HX, Cao YJ, Zhang Y, Terzija V. Quantitative synergy assessment of regional wind-solar energy resources based on MERRA reanalysis data. Appl Energy 2018;216:172–82.
[26] Liu Y, Xiao LY, Wang HF, Dai ST, Qi ZP. Analysis on the hourly spatiotemporal complementarities between China's solar and wind energy resources spreading in a wide area. Sci China Technol Sci 2013;56:683–92.
[27] Kozarcanin S, Liu HL, Andresen GB. 21st century climate change impacts on key properties of a large-scale renewable-based electricity system. Joule 2019;3:992–1005.
[28] Palutikof JP, Cook HF, Davies TD. Effects of geographical dispersion on wind turbine performance in England - a simulation. Atmos Environ Part a-General Topics 1990;24:213–27.
[29] Landberg L. Short-term prediction of the power production from wind farms. J Wind Eng Ind Aerod 1999;80:207–20.
[30] Kiss P, Janosi IM. Limitations of wind power availability over Europe: a conceptual study. Nonlinear Process Geophys 2008;15:803–13.
[31] Katzenstein W, Fertig E, Apt J. The variability of interconnected wind plants. Energy Pol 2010;38:4400–10.
[32] Martin CMS, Lundquist JK, Handschy MA. Variability of interconnected wind plants: correlation length and its dependence on variability time scale. Environ Res Lett 2015;10.
[33] Mills A, Ahlstrom Mark, Michael Brower, Ellis Abraham, George Ray, Hoff Tom, et al. Understanding variability and uncertainty of photovoltaics for integration with the electric power system. Berkeley, California: Lawrence Berkeley National Laboratory; 2009.
[34] Murata A, Yamaguchi H, Otani K. A method of estimating the output fluctuation of many photovoltaic power generation systems dispersed in a wide area. Electr Eng Jpn 2009;166:9–19.
[35] 15km Wind Resource Data Technical Report (Inner). China Meteorological Administration: National Climate Center; 2018.
[36] Association CWE. Breif report on China's wind power hoisting capacity in. 2018. 2019.
[37] Zhu QZ. Invesitigation on the power reduction factor of wind farms (in Chinese)10. Wind Energy Industry; 2019.
[38] Tang WJ, Qin J, Yang K, Liu SM, Lu N, Niu XL. Retrieving high-resolution surface solar radiation with cloud parameters derived by combining MODIS and MTSAT data. Atmos Chem Phys 2016;16:2543–57.
[39] Campana PE, Li H, Zhang J, Zhang R, Liu J, Yan J. Economic optimization of photovoltaic water pumping systems for irrigation. Energy Convers Manag 2015;95:32–41.
[40] Elia CP, Zhang Y, Anders L, Li HL, Yan JY. An open-source platform for simulation and optimization of clean energy technologies. 8th International Conference on Applied Energy (Icae2016) 2017;105:946–52.
[41] Yan JY, Yang Y, Campana PE, He JJ. City-level analysis of subsidy-free solar photovoltaic electricity price, profits and grid parity in China. Nature Energy 2019;4:709–17.
[42] Zhang Y, Campana PE, Lundblad A, Wang L, Yan JY. The influence of photovoltaic models and battery models in system simulation and optimization. 8th International Conference on Applied Energy (Icae2016) 2017;105:1184–91.
[43] Dee DP, Uppala SM, Simmons AJ, Berrisford P, Poli P, Kobayashi S, et al. The ERA-Interim reanalysis: configuration and performance of the data assimilation system. Q J R Meteorol Soc 2011;137:553–97.
[44] Klein SA. Calculation of monthly average insolation on tilted surfaces. Sol Energy 1977;19:325–9.
[45] Hay JE. Calculation of monthly mean solar-radiation for horizontal and inclined surfaces. Sol Energy 1979;23:301–7.
[46] Implementation opinions on promoting the construction of multi-energy complementary integration optimization demonstration project (in Chinese). National Development and Reform Commission NEA. 2017.
[47] Dai JC, Yang X, Wen L. Development of wind power industry in China: a comprehensive assessment. Renew Sustain Energy Rev 2018;97:156–64.
[48] Qi Y, Dong WJ, Dong CG, Huang CW. Understanding institutional barriers for wind curtailment in China. Renew Sustain Energy Rev 2019;105:476–86.
[49] Dong CG, Qi Y, Dong WJ, Lu X, Liu TL, Qian S. Decomposing driving factors for wind curtailment under economic new normal in China. Appl Energy 2018;217:178–88.
[50] Lu X, McElroy MB, Peng W, Liu SY, Nielsen CP, Wang HK. Challenges faced by China compared with the US in developing wind power. Nature Energy 2016;1.
[51] Davis SJ, Lewis NS, Shaner M, Aggarwal S, Arent D, Azevedo IL, et al. Net-zero emissions energy systems. Science 2018;360:1419.